

## **Entropy Generation on MHD Viscoelastic Nanofluid over a Stretching Surface**

M. Zakaria, Azza M. Moshen

*Department of Mathematics, Faculty of Science, Al-Baha University, Al-Aqiq, P.O. Box 1988, Kingdom of Saudi Arabia.*

---

**Abstract:** *This paper deals with the double-diffusive boundary layer flow of non-Newtonian nano-fluid over a stretching sheet. In this model, where binary nano-fluid is used, the Brownian motion and thermophoresis are classified as the main mechanisms which are responsible for the enhancement of the convection features of the nanofluid. By means of the successive approximation method the governing equations for momentum and energy have been solved. Nevertheless, these boundary-value problems can be solved correctly using expansions solutions, and we present the formulation that makes this possible (in essence, an application of Duhamel's principle). The solutions obtained by this new approach are shown to agree identically with those obtained by using numerical method solutions. Graphical display of the numerical examine are performed to illustrate the influence of various flow parameters on the velocity, temperature, concentration, reduced Nusselt, reduced Sherwood and reduced nano-fluid Sherwood number distributions. The present study has many applications in coating and suspensions, movement of biological fluids, cooling of metallic plate, melt-spinning, heat exchangers technology, and oceanography. Some important findings reported in this work reveals that expansion solutions effect of momentum equations have significant impact in controlling the rate of velocity in the boundary layer region.*

---

### **I. Introduction**

Boundary layer behaviour over a moving continuous solid surface is an important type of flow occurring in a number of engineering processes. To be more specific, heat-treated materials travelling between a feed roll and a wind-up roll, aerodynamic extrusion of plastic sheets, glass fiber and paper production, cooling of an infinite metallic plate in a cooling path, manufacturing of polymeric sheets are examples for practical applications of continuous moving flat surfaces. Since the pioneering work of Sakiadis [1], various aspects of the problem have been investigated by many authors. Mass transfer's analyses at the stretched sheet were enclosed in their studies by Erickson et al. [2] and relevant experimental results were reported by Tsou et al. [3] regarding several aspects for the flow and heat transfer boundary layer problems in a continuously moving sheet. Crane [4] and Gupta and Gupta [5] have analyzed the stretching problem with constant surface temperature while Soundalgekar [6] investigated the Stokes problem for a viscoelastic fluid. This flow was examined by Siddappa and Khapate [7] for a special class of non-Newtonian fluids known as second-order fluids which are viscoelastic in nature.

Crane [8] considered the laminar boundary layer flow of a Newtonian fluid caused by a flat elastic sheet whose velocity varies linearly with the distance from the fixed point of the sheet. Rajagopal et al. [9] and Chang [10] presented an analysis on flow of viscoelastic fluid over stretching sheet. Heat transfer cases of these studies have been considered by Dandapat and Gupta [11] and Vajravelu and Rollins [12], while flow of viscoelastic fluid over a stretching surface under the influence of uniform magnetic field has been investigated by Andersson [13].

Heat transfer is a widespread phenomenon in the nature which exists due to temperature difference between objects or within the same body. Fourier's law of heat conduction law [14] is successfully for understanding the phenomena of heat transfer. However, the main shortcoming of the Fourier's laws contradicts the principle of causality. The propagation speed of heat disturbance is finite by introducing the thermal relaxation time in the Fourier's model [15]. Moreover, Christov [16] modified the time derivative in the Maxwell-Cattaneo model with the Oldroyd upper-convected derivative which successful preserves the material-invariant formulation. For the incompressible fluid with the Cattaneo-Christov heat conduction model, Tibullo and Zampoli [17] proved the uniqueness of the solution. Han et al. [18] studied coupled flow and heat transfer in viscoelastic fluid with Cattaneo-Christov heat flux model. He successfully studied the effects of the relevant parameters on the temperature and velocity. Mustafa [19] explored the rotating flow of Maxwell fluid over a linear stretching sheet with the Cattaneo-Christov heat flux. Hayat et al. [20,21] studied the flow over a stretching sheet with variable thickness and MHD flow of Oldroyd-B fluid with homogeneous-heterogeneous reactions with Cattaneo-Christov heat flux, respectively. Recently, the interest has been extended to the problem

of the flow and heat transfer over sheet by utilizing CattaneoChristov heat flux model. However, the model has seldom been used to study coupled flow and heat transfer of boundary layer in viscoelastic fluid.

Heat and mass transfers simultaneously affecting each other will also cause a cross-diffusion effect. The mass transfer caused by the temperature gradient is called the Soret effect, while the heat transfer caused by the concentration gradient is called the Dufour effect. Due to much attention in many fields that includes solid state physics, chemical engineering, geophysics, and oceanography, the research on the double\_diffusive convective boundary layer has become a topic of great interest. Pop and Ingham [21] gave the detailed review about the topic of thermo diffusion effect. Investigators [22–24] have reported and studied results for the fluids which have very light molecular weight due to the importance of thermal diffusion and diffusion thermo effects of these fluids. Mansour et al. [25] presented the effects of chemical reaction and thermal stratification on free convective heat and mass transfer over a vertical stretching surface embedded in a porous media considering the Soret and Dufour numbers in the presence of MHD. The heat and mass transfer on Hiemenz flow through porous medium onto a stretching surface was investigated by Tsai and Huang [26] for Soret and Dufour effects. The numerical solution of MHD free convective flow under Soret and Dufour effects over a stretching sheet immersed in a porous medium was analyzed by Bég et al. [27]. Kuznetsov and Nield [28] presented the analysis of the double diffusion free convection boundary layer flow of a nanofluid in porous media. Later on, Khan and Aziz [29] employed the same idea to study the double\_diffusive natural convection from a vertical plate under prescribed surface heat, solutal and nanoparticle fluxes. W.A. Khan et al. [30] studied the thermo diffusion effect on free convective boundary layer flow of a nanofluid past a convectively heated vertical plate in the presence of momentum slip. Recently, F.G. Awad et al. [31] examined numerically the thermodiffusion effects on magneto fluid flow over a stretching sheet.

In real situations in nano-fluids, the base fluid do not satisfy the properties of Newtonian fluids, hence it is more justified to consider them as viscoelastic fluids, e.g., Ethylene glycol- $Al_2O_3$ , Ethylene glycol- $CuO$  and Ethylene glycol- $ZnO$  are some examples of viscoelastic nano-fluids. In the present study we extend the work of Khan and Pop [32] using a modification of the model of Buongiorno [33] to the case of a binary nano-fluid. With the idea of creating a detailed comparison with cross-diffusion effects for the regular fluids and the cross-diffusion effects peculiar to nano-fluids, a new approach in nano-fluids to cross-diffusion is made and also when the base fluid of the nano-fluid contains solute (e.g. salt) as well as nano-particles investigation of the interaction between these effects is carried out at the same time. The outcome is that we are investigating a sort of triple-diffusion problem involving heat, the nanoparticles and the solute. Here, the base fluid is taken as second grade fluid. To our best of knowledge, no studies have far been investigated to analyze the thermo diffusion effects on the boundary layer flow of viscoelastic nano-fluid over a permeable stretching sheet. The solutions of the resulting non-linear equations are solved by using the successive approximation method. The effects of the embedded flow controlling parameters on the fluid velocity, temperature, and nanoparticle concentration, heat transfer rate, and the nanoparticle volume fraction rate have been demonstrated graphically and discussed. A comparative study is also given.

## II. Formulation Of The Problem

We consider two-dimensional incompressible boundary layer flow optically dense nanofluid over a convectively heated permeable stretching sheet located at  $y = 0$ . The sheet is stretched through two equal and opposite forces along x-axis by keeping the origin fixed with the velocity  $U_o = ax^m$ , at  $t = 0$ , moving wedge and flat plate. A uniform magnetic field of strength  $B_0$  is assumed to be applied normal to the stretching surface. The magnetic Reynolds number is taken to be small and therefore the induced magnetic field and electric field are neglected. Heat transfer analysis based for fixed volume fraction of nanoparticles is carried out in the presence of thermal radiation, Brownian motion, thermophoresis and viscous dissipation effects. The sheet surface is heated by a hot fluid with uniform temperature  $T_f$  and the convective heat transfer coefficient  $h_f$  as shown in Fig. 1:

Following the Zakaria [34], the unsteady boundary layer equations governing the two-dimensional incompressible stagnation point flow of nanofluid can be written as

$$\frac{\partial u}{\partial x} + \frac{\partial v}{\partial y} = 0, \tag{1}$$

$$\left(\frac{\partial u}{\partial t} + u \frac{\partial u}{\partial x} + v \frac{\partial u}{\partial y}\right) = v \frac{\partial^2 u}{\partial y^2} - \frac{\sigma B_0^2}{\rho_f} u - \frac{v}{k} u, \\ -K_o \left(\frac{\partial^3 u}{\partial t \partial^2 y} + u \frac{\partial^3 u}{\partial x \partial^2 y} + v \frac{\partial^3 u}{\partial^3 y} + \frac{\partial u}{\partial x} \frac{\partial^2 u}{\partial y^2} - \frac{\partial u}{\partial y} \frac{\partial^2 u}{\partial x \partial y}\right), \tag{2}$$

$$\left(\frac{\partial T}{\partial t} + u \frac{\partial T}{\partial x} + v \frac{\partial T}{\partial y}\right) = \alpha \frac{\partial^2 T}{\partial y^2} + \tau \left[ D_B \frac{\partial N}{\partial y} \frac{\partial T}{\partial y} + \frac{D_T}{T_\infty} \left(\frac{\partial T}{\partial y}\right)^2 \right], \tag{3}$$

$$\left(\frac{\partial N}{\partial t} + u \frac{\partial N}{\partial x} + v \frac{\partial N}{\partial y}\right) = D_B \frac{\partial^2 N}{\partial y^2} + \frac{D_T}{T_\infty} \frac{\partial^2 T}{\partial y^2}, \quad (4)$$

where  $u$  and  $v$  are the component of velocity along the  $x$  and  $y$  directions,  $\rho_f$  is the density of the fluid  $K_o$  is the coefficient of elastic velocity of fluid,  $T$  is the temperature of the fluid in the boundary layer,  $N$  is the nanoparticle volume fraction,  $\rho_p$  is the nanoparticle density,  $\mu$  is the absolute viscosity of the base fluid,  $\nu$  is the kinematic viscosity of the base fluid,  $\alpha = k/(\rho C)_f$  is the thermal diffusivity of the fluid,  $\tau(= (\rho C)_p/(\rho C)_f)$  is the ratio of effective heat capacity of the nanoparticle material  $T_o$  heat capacity of the fluid,  $D_{TC}$  and  $D_{CT}$  are the Dufour and Soret type diffusivity,  $D_S$  is the solutal diffusivity,  $D_B$  and  $D_T$  are the Brownian diffusion coefficient and the thermophoresis diffusion coefficient,  $T_\infty$  the free stream temperature,  $C_p$  is the specific heat at constant pressure, and  $g, k$  are the acceleration due to gravity, the thermal conductivity of the fluid respectively,  $B_o$  is the applied magnetic field along  $y$  direction,  $k$  is porosity parameter, and  $\sigma$  is the electrical conductivity. The boundary and initial conditions imposed on Eqs. (1)–(4), are

$$\begin{cases} y = 0 & u = ax^m e^{\omega t}, & v = -amx^{m-1} - V_o e^{\omega t}, & t \geq 0, \\ y = 0, & T - T_\infty = T_o x^m e^{\omega t}, & & t \geq 0, \\ y = 0, & N - N_\infty = N_w x^m e^{\omega t}, & & t \geq 0, \\ y \rightarrow \infty, & u \rightarrow 0, & T \rightarrow T_\infty, & N \rightarrow N_\infty \end{cases} \quad (5)$$

where  $a$ , and  $\omega$  are constants,  $V_o$  is the velocity condition at the surface,  $T_o$  is the mean temperature of the surface,  $T_\infty$  is the temperature condition far away from the surface, and  $m$  is the power law exponent,  $N_o$  is the mean nanoparticle volume fraction.

We introduce the following non-dimensional quantities

$$\begin{cases} x^* = \sqrt{\frac{a}{\nu}} x, & y^* = \sqrt{\frac{a}{\nu}} y, & t^* = at, & M^* = \sqrt{\frac{\sigma B_o^2}{a \rho_f}}, & f_\omega = \frac{V_o}{\sqrt{a\nu}}, \\ u^* = \frac{u}{\sqrt{a\nu}}, & v^* = \frac{v}{\sqrt{a\nu}}, & P = \frac{\rho C_p \nu}{\lambda}, & k^* = \frac{ak}{\nu}, & \alpha^* = \frac{\alpha}{\sqrt{a\nu}}, \\ \omega^* = \frac{\omega}{a}, & K_o^* = \frac{a}{\nu}, & N^* = \frac{(N - N_\infty)}{N_o}, & T^* = \frac{(T - T_\infty)}{T_o}, \end{cases}$$

where  $f_\omega$  is the mass transfer, and  $P$  is the Prandtl number  $k^*$  is the porosity parameter,  $M^*$  is the Hartmann number.

The mass transfer parameter  $f_\omega$  is positive for injection and negative for suction.

Invoking the non-dimensional quantities above, Eqs. (1)–(5), are reduced to the non-dimensional equations, dropping the asterisks for convenience,

$$\frac{\partial u}{\partial x} + \frac{\partial v}{\partial y} = 0, \quad (6)$$

$$\left(\frac{\partial u}{\partial t} + u \frac{\partial u}{\partial x} + v \frac{\partial u}{\partial y}\right) = \frac{\partial^2 u}{\partial y^2} - M^2 u - \frac{1}{k} u, \\ -K_o \left(\frac{\partial^3 u}{\partial t \partial^2 y} + u \frac{\partial^3 u}{\partial x \partial^2 y} + v \frac{\partial^3 u}{\partial^3 y} + \frac{\partial u}{\partial x} \frac{\partial^2 u}{\partial y^2} - \frac{\partial u}{\partial y} \frac{\partial^2 u}{\partial x \partial y}\right), \quad (7)$$

$$\left(\frac{\partial T}{\partial t} + u \frac{\partial T}{\partial x} + v \frac{\partial T}{\partial y}\right) = \frac{1}{P} \frac{\partial^2 T}{\partial y^2} + N_b \frac{\partial N}{\partial y} \frac{\partial T}{\partial y} + N_t \left(\frac{\partial T}{\partial y}\right)^2, \quad (8)$$

$$\left(\frac{\partial N}{\partial t} + u \frac{\partial N}{\partial x} + v \frac{\partial N}{\partial y}\right) = \frac{1}{L_e} \frac{\partial^2 N}{\partial y^2} + \frac{N_t}{L_e N_b} \frac{\partial^2 T}{\partial y^2}, \quad (9)$$

$L_e = \nu/D_B$  is the Lewis number,  $N_b = \tau D_B N_o/\nu$  is Brownian motion parameter and  $N_t = \tau D_T T_o/T_\infty \nu$  is the thermophoresis parameter

Their corresponding boundary conditions are

$$\begin{cases} y = 0 & u = x^m e^{\omega t}, & v = -x^{m-1} e^{\omega t} f_\omega, & t \geq 0, \\ y = 0, & T = x^m e^{\omega t}, & & t \geq 0, \\ y = 0, & N = x^m e^{\omega t}, & & t \geq 0, \\ y \rightarrow \infty, & u \rightarrow 0, & T \rightarrow 0, & N \rightarrow 0 \end{cases} \quad (10)$$

**III. The Method Of Successive Approximations**

A process of successive approximations [35] will integrate the unsteady boundary layer equations (6)–(9). Selecting a system of coordinates which is at rest with respect to the plate and that the magnetohydrodynamic flow of fluid moves with respect to the plane surface, we can assume that the velocities  $u, v$ , the temperature  $T$ , and the nanoparticle volume fraction  $N$  possess a series solutions of the form:

$$\begin{aligned}
 u(x, y, t) &= \sum_{i=0}^{\infty} u_i(x, y, t), & v(x, y, t) &= \sum_{i=0}^{\infty} v_i(x, y, t) \\
 T(x, y, t) &= \sum_{i=0}^{\infty} T_i(x, y, t), & N(x, y, t) &= \sum_{i=0}^{\infty} N_i(x, y, t)
 \end{aligned}
 \tag{11}$$

where  $u_i(x, y, t) = O(\varepsilon^i)$ ,  $i$ -integer and  $\varepsilon$  is a small number.

Each term in the series (11) must satisfy the boundary continuity equation (10)

$$\frac{\partial u_i}{\partial x} + \frac{\partial v_i}{\partial y} = 0, \quad i = 1, 2.
 \tag{12}$$

Substituting the series (11) into Eqs. (7)-(9) and setting equal to zero terms of the same order, one obtains equations for finding components of the series (11)

$$\frac{\partial^2 u_o}{\partial y^2} - K_o \frac{\partial^3 u_o}{\partial t \partial^2 y} - \frac{\partial u_o}{\partial t} - M^2 u_o - \frac{1}{k} u_o = 0,
 \tag{13}$$

$$\frac{\partial^2 T_o}{\partial y^2} = P \frac{\partial T_o}{\partial t},
 \tag{14}$$

$$\frac{\partial^2 N_o}{\partial y^2} + \frac{N_t}{N_b} \frac{\partial^2 T_o}{\partial y^2} - L_e \frac{\partial N_o}{\partial t} = 0,
 \tag{15}$$

$$\begin{aligned}
 \frac{\partial^2 u_1}{\partial y^2} - K_o \frac{\partial^3 u_1}{\partial t \partial^2 y} - \frac{\partial u_1}{\partial t} - M^2 u_1 - \frac{1}{k} u_1 &= \left( u_o \frac{\partial u_o}{\partial x} + v_o \frac{\partial u_o}{\partial y} \right), \\
 &+ K_o \left( u_o \frac{\partial^3 u_o}{\partial x \partial^2 y} + v_o \frac{\partial^3 u_o}{\partial^3 y} + \frac{\partial u_o}{\partial x} \frac{\partial^2 u_o}{\partial y^2} - \frac{\partial u_o}{\partial y} \frac{\partial^2 u_o}{\partial x \partial y} \right),
 \end{aligned}
 \tag{16}$$

$$\frac{\partial^2 T_1}{\partial y^2} - P \frac{\partial T_1}{\partial t} = P \left[ u_o \frac{\partial T_o}{\partial x} + v_o \frac{\partial T_o}{\partial y} - N_B \frac{\partial N_o}{\partial y} \frac{\partial T_o}{\partial y} - N_t \left( \frac{\partial T_o}{\partial y} \right)^2 \right],
 \tag{17}$$

$$\frac{\partial^2 N_1}{\partial y^2} + \frac{N_t}{N_b} \frac{\partial^2 T_1}{\partial y^2} - L_e \frac{\partial N_1}{\partial t} = L_e \left[ u_o \frac{\partial N_o}{\partial x} + v_o \frac{\partial N_o}{\partial y} \right],
 \tag{18}$$

Combining Eq. (11) and Eq. (10), we have the corresponding boundary conditions

$$\begin{cases}
 y = 0 & u_o = x^m e^{\omega t}, & u_i = 0, & i = 1, 2, \dots & t \geq 0, \\
 y = 0 & v_o = x^{m-1} e^{\omega t} f_\omega, & v_i = 0, & i = 1, 2, \dots & t \geq 0, \\
 y = 0, & T_o = x^m e^{\omega t}, & T_i = 0, & i = 1, 2, \dots & t \geq 0, \\
 y = 0, & N_o = x^m e^{\omega t}, & N_i = 0, & i = 1, 2, \dots & t \geq 0, \\
 y \rightarrow \infty, & u \rightarrow 0, & T \rightarrow 0, & & N \rightarrow 0.
 \end{cases}
 \tag{19}$$

In the following analysis, the first two terms in the series solution (11) will be retained. It is known fact [35] that such solution is satisfactory in the phases of the non-periodic motion after it has been started from rest (till the moment when the first separation of boundary layer occurs) and in the case of periodic motion when the amplitude of oscillation is small. Higher-order approximations  $u_3$ , can be obtained easy in principle. However, the complexity of the method of successive approximations increases rapidly as higher approximations are considered. It is also known that third and higher terms series solutions give small changes in the results compared with the two terms series solutions.

**IV. Solution Of The Problem**

Let us suppose that the exact solutions of the differential equations (13)-(15), is of the form:

$$u_o(x, y, t) = x^3 e^{\omega t} f_o'(y)
 \tag{20}$$

$$T_o(x, y, t) = x^2 e^{\omega t} \theta_o(y)
 \tag{21}$$

$$N_o(x, y, t) = x^2 e^{\omega t} \phi_o
 \tag{22}$$

Using Eq. (12)

$$v_o(x, y, t) = -3x^2 e^{\omega t} f_o(y),
 \tag{23}$$

from Eqs. (13)- (15) and using Eqs. (20)–(22) one obtains the differential equations of the unknown functions  $f_o(y), \theta(y)$  and  $\phi(y)$  and the corresponding boundary conditions

$$f_o''' - k_1^2 f_o' = 0, \tag{24}$$

$$\theta_o'' - \omega P \theta_o = 0, \tag{25}$$

$$\phi'' - \omega L_e \phi = \frac{N_t}{N_b} \theta'', \tag{26}$$

$$\begin{cases} y = 0 & f_o = -f_\omega, & f_o' = 1, & t \geq 0, \\ y = 0, & \theta_o = 1, & \phi_o = 1, & t \geq 0 \\ y \rightarrow \infty, & f_o' \rightarrow 0, & \theta_o \rightarrow 0, & \phi_o \rightarrow 0 \end{cases} \tag{27}$$

where  $k_1^2 = \frac{(\omega + M^2 + 1/k)}{1 - \omega K_o}$ .

The solutions of the system (24)–(26) are of the form, taking into account the boundary conditions (27)

$$f_o(y) = \frac{1}{k_1} (1 - e^{-k_1 y}) - f_\omega \tag{28}$$

$$\theta_o(y) = e^{-\sqrt{\omega P} y} \tag{29}$$

$$\phi_o(y) = \ell_1 e^{-\sqrt{\omega L_e} y} + (1 - \ell_1) e^{-\sqrt{\omega P} y}, \tag{30}$$

Where  $\ell_1 = \frac{N_b(P - L_e) - N_t}{N_b \omega(P - L_e)}$ .

Assuming the solutions of the differential equation (16) is of the form

$$u_1(x, y, t) = x^5 e^{2\omega t} f_1'(y). \tag{31}$$

We can obtain an exact solution of equation (17) and (18) if we consider the case  $m = 4$

$$T_1(x, y, t) = x^4 e^{2\omega t} \theta_1(y) \tag{32}$$

$$N_1(x, y, t) = x^4 e^{2\omega t} \phi_1 \tag{33}$$

and using Eqs. (31)–(33) one obtains from Eqs. (16)–(18) the differential equations for  $f_1, \theta_1$  and  $\phi_1$  and the corresponding boundary conditions

$$f_1'' - k_3^2 f_1' = \frac{3}{1 - 2\omega} [f_o'^2 - f_o f_o'' + K_o (2f_o' f_o''' - f_o f_o'''' - (f_o'')^2)], \tag{34}$$

$$\theta_1'' - 2\omega P \theta_1 = P [2f_o' \theta_o - 3f_o \theta_o' - N_b \phi_o' \theta_o' - N_t (\theta_o')^2], \tag{35}$$

$$\phi_1'' - 2\omega L_e \phi_1 = L_e [2f_o' \phi_o - 3f_o \phi_o'] - \frac{N_t}{N_b} \theta_1'', \tag{36}$$

where  $k_3^2 = \frac{(2\omega + M^2 + 1/k)}{1 - 2\omega K_o}$  and  $k_4^2 = \frac{2\omega L_e N_b}{N_b + N_t}$ .

$$\begin{cases} y = 0 & f_1 = 0, & f_1' = 0, & t \geq 0, \\ y = 0, & \theta_1 = 0, & \phi_1 = 0, & t \geq 0 \\ y \rightarrow \infty, & f_1' \rightarrow 0, & \theta_1 \rightarrow 0, & \phi_1 \rightarrow 0 \end{cases} \tag{37}$$

Using Eqs. (28)–(30) one obtains the solutions of the system (34)–(37)

$$f_1'(y) = \ell_{11} e^{-k_3 y} + \ell_{12} e^{-k_1 y} + \ell_{13} e^{-2k_1 y} \tag{38}$$

$$\theta_1(y) = \ell_{21} e^{-\sqrt{2\omega P} y} + \ell_{22} e^{-\sqrt{\omega P} y} + \ell_{23} e^{-(k_1 + \sqrt{\omega P}) y} + \ell_{24} e^{-\sqrt{\omega(P + L_e)} y}, \tag{39}$$

$$\begin{aligned} \phi_1(y) = & \ell_{31} e^{-\sqrt{2\omega L_e} y} + \ell_{32} e^{-\sqrt{\omega L_e} y} + \ell_{33} e^{-\sqrt{\omega P} y} + \ell_{34} e^{2\omega P} + \ell_{35} e^{-(k_1 + \sqrt{\omega L_e}) y} \\ & + \ell_{36} e^{-\sqrt{\omega(P + L_e)} y} + \ell_{37} e^{-(k_1 + \sqrt{\omega L_e}) y} \end{aligned} \tag{40}$$

where

$$\begin{aligned} \ell_{11} = & -(\ell_{12} + \ell_{13}), \ell_{12} = \frac{3(1+k_1 f_\omega)[K_o k_1^2 - 1]}{(1-2\omega)(k_1^2 - k_3^2)}, \ell_{13} = \frac{6}{(1-2\omega)(4k_1^2 - k_3^2)} \\ \ell_{21} = & -(\ell_{22} + \ell_{23} + \ell_{24}), \ell_{22} = \frac{\sqrt{\omega P}(1 - k_1 f_\omega)}{\omega k_1^2}, \ell_{23} = \frac{P\sqrt{\omega P}}{k_1(k_1^2 + 2k_1\sqrt{\omega P} - \omega P)}, \\ \ell_{24} = & \frac{PN_b \ell_1 \sqrt{PL_e}}{L_e - P}, \ell_{31} = -(\ell_{32} + \ell_{33} + \ell_{34} + \ell_{35} + \ell_{36} + \ell_{37}) \\ \ell_{32} = & \frac{3\ell_1 \sqrt{L_e}(k_1 f_\omega - 1)}{k_1 \sqrt{\omega}}, \ell_{33} = \frac{N_t P \ell_{22}}{N_b(2L_e - P)}, \ell_{34} = \frac{N_t P \ell_{21}}{N_b(L_e - P)}, \ell_{35} = \frac{N_t \ell_{23}(k_1 + \sqrt{\omega P})^2}{N_b(2\omega L_e - k_1 - \sqrt{\omega P})}, \ell_{36} \\ = & \frac{N_t \ell_{23}(P + L_e)}{N_b(L_e - P)}, \\ \ell_{37} = & \frac{\ell_1 L_e (2k_1 - 3\sqrt{\omega L_e})}{k_1(2\omega L_e - k_1 - \sqrt{\omega L_e})}. \end{aligned}$$

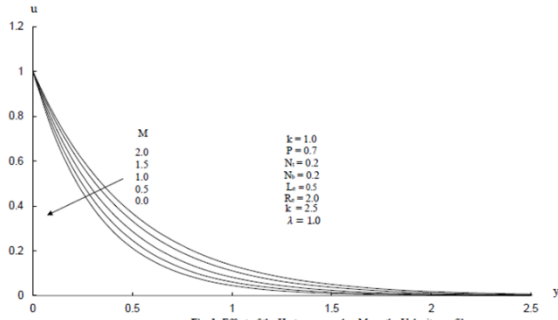


Fig. 1: Effect of the Hartmann number M on the Velocity profile

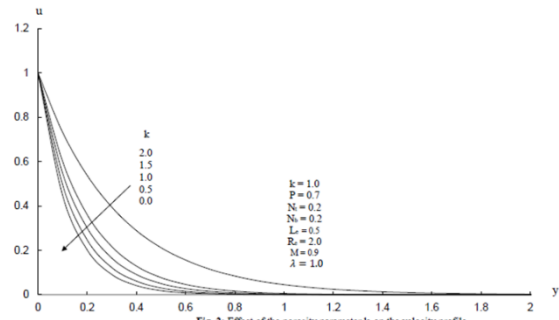


Fig. 2: Effect of the porosity parameter k on the velocity profile

### V. Entropy Generation Analysis

For natural convection heat transfer in a fluid saturated porous medium, entropy generation rates due to heat transfer and fluid flow friction are expressed by the following expressions according to Bejan [36, 37]:

$$\dot{S}_{gen} = \dot{S}_T + \dot{S}_V + \dot{S}_C \tag{41}$$

$$\dot{S}_T = \frac{\kappa}{T_\infty^2} \left( \frac{\partial T}{\partial y} \right)^2 \tag{42}$$

$$\dot{S}_V = \frac{\mu}{T_\infty} \left( 2 \left( \frac{\partial u}{\partial x} \right)^2 + 2 \left( \frac{\partial v}{\partial y} \right)^2 + \left( \frac{\partial u}{\partial y} + \frac{\partial v}{\partial x} \right)^2 \right) + \frac{1}{T_\infty} \left( \sigma B^2 + \frac{\mu}{k} \right) u^2 \tag{43}$$

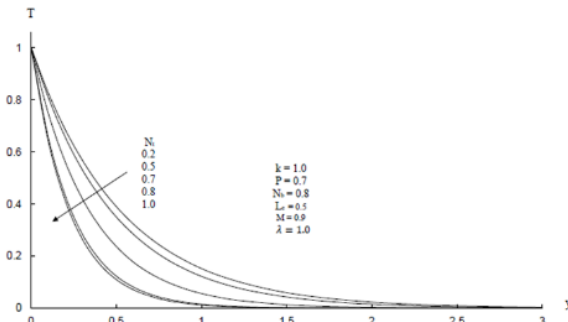


Fig. 3: Effect of the thermophoresis parameter N on Temperature distribution

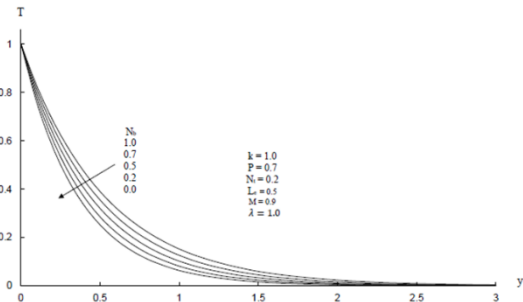


Fig. 4: Effect of the Brownian motion parameter N\_0 on Temperature distribution

$$\dot{S}_C = \frac{RD_B}{N_\infty} \left( \frac{\partial N}{\partial y} \right)^2 + \frac{RD_B}{T_\infty} \left( \frac{\partial T}{\partial y} \frac{\partial N}{\partial y} + \frac{\partial N}{\partial x} \frac{\partial T}{\partial x} \right), \tag{44}$$

The first term on the right hand side of Eq. (41) represents the entropy generation rate due to heat transfer irreversibility and is calculated by Eq. (42). The second term indicates the entropy generation rate due to viscous dissipation effects expressed by Eq. (43).

(43). It's worthy to mention that the first term in Eq. (43) is important when the permeability of the medium is large and the flow tends to behave as a non-pours medium flow, while the second term in this equation is the entropy generation rate due to viscous effects for pours medium flows which is important for low speed flows. For intermediate the permeability of the medium values both of the mentioned terms in Eq. (43) are important and have to be considered for calculation of the viscous entropy generation rate. The last term in the right hand side of Eq. (41) indicates the entropy generation rate due to concentration gradients and is defined by Eq. (44).

Using the dimensionless variables defined in Section 2, Eq. (41) can be rewritten in the dimensionless form as follows:

$$\dot{S}_{gen} = Re\theta'^2 + \frac{ReBr}{\Omega} \left( (M^2 + k)u^2 + u'^2 \right) + Re\lambda_1 \left( \frac{\chi}{\Omega} \right) \left( \left( \frac{\chi}{\Omega} \right) N^2 + \theta'N' \right) \tag{45}$$

where  $R_e$  and  $B_r$  are the Reynolds number, Reynolds number is used to check whether the flow is laminar or turbulent, and Brinkmann number, the Brinkman number is a dimensionless number related to heat conduction from a surface to a flowing viscoelastic fluid, respectively,  $\Omega$  is the dimensionless temperature difference,  $R$  is the fluid constant,  $\chi$  and  $\lambda_1$  are the constant parameters. These number are given in the following form

$$R_e = \frac{aL^2}{\nu}, \quad B_r = \frac{\mu u^2}{\kappa T}, \quad \Omega = \frac{T_0 - T_\infty}{T_\infty}, \quad \chi = \frac{N_0 - N_\infty}{N_\infty}, \quad \lambda_1 = \frac{RD_B C_\infty}{\kappa},$$

L is the characteristic length, e.g. the diameter of the particle and  $u, \theta$  and  $N$  are given by:

$$u = x^3 e^{\omega t} (u_0 + x^2 e^{\omega t} u_1), \theta = x^2 e^{\omega t} (T_0 + x^2 e^{\omega t} T_1)$$

$$N = x^2 e^{\omega t} (N_0 + x^2 e^{\omega t} N_1)$$

### VI. Results And Discussion

In this section, the numerical results of all the physical parameters of interest are plotted for velocity profile, temperature profile, nano-particle concentration and entropy generation. For this purpose Figs. 1, 2, 3, 4, 5, 6, 7, 8 and 9 are sketched for Hartmann number (M), porous parameter (k), Brownian motion parameter ( $N_b$ ), thermophoresis parameter ( $N_t$ ), Lewis number ( $L_e$ ), Reynolds number ( $R_e$ ) and Brinkman number ( $B_r$ ). The step sizes chosen  $y = 0.0001$  and  $y_\infty = 3$  at their given boundary conditions. Furthermore.

Figures 1 and 2 are sketched for velocity profile. From Fig. 1 one can observe that due to the influence of Hartmann number (M), the velocity of the fluid accelerates, while the behavior of velocity remains same when the porosity parameter (k) increases as shown in Fig. 2. Figure 3 is plotted for different values of thermophoresis parameter ( $N_t$ ). From this figure we can scrutinize that due to the influence of thermophoresis parameter ( $N_t$ ), temperature profile behaves as a decreasing function. It can be visualized from Fig. 4 that when the Brownian motion parameter  $N_b$  increases, then it helps to diminish the temperature profile.

Figures 5, 6 and 7 are drawn for nano-particle concentration. It is clear from Fig. 5 that with the

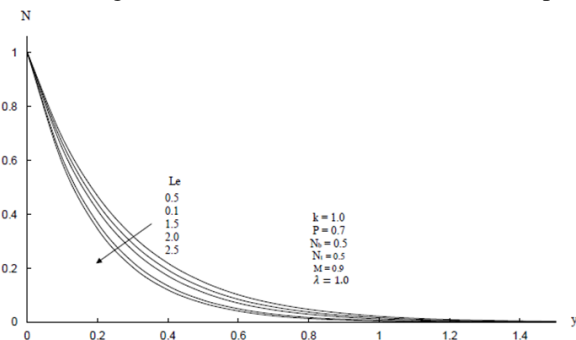


Fig. 5: Effect of the Lewis number  $L_e$  on nanoparticle volume fraction

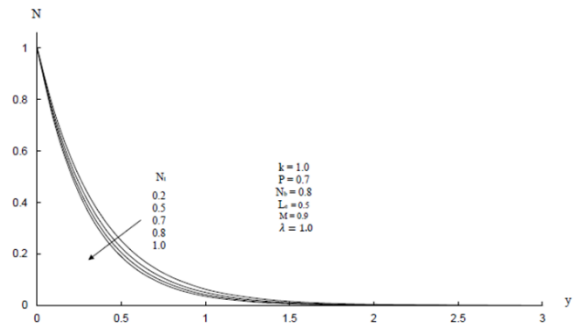


Fig. 6: Effect of the thermophoresis parameter  $N_t$  on nanoparticle volume fraction

increment in Lewis number ( $L_e$ ), concentration profile decreases. It can be also observed from Figs. 6 and 7 that Brownian motion parameter and thermophoresis parameter depicts opposite behavior on concentration profile. The effect of Brinkman number ( $B_r$ ) on entropy generation is illustrated in Fig. 8. It can be visualized from this figure that due to the increment in Brinkman number ( $B_r$ ), the entropy generation number ( $S_{gen}$ ) increases. It

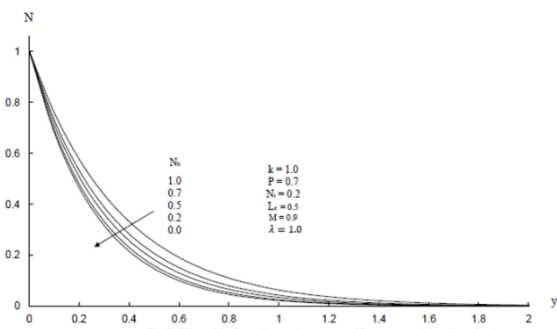


Fig. 7: Effect of the Brownian motion parameter  $N_b$  on nanoparticle volume fraction

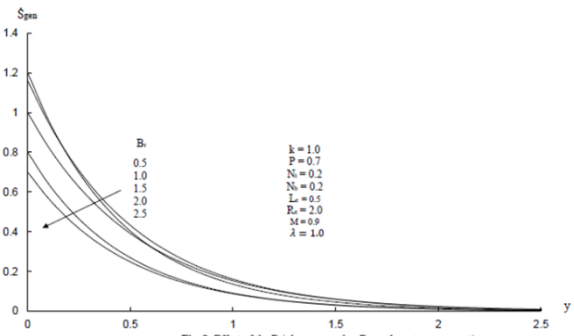


Fig. 8: Effect of the Brinkmann number  $B_r$  on the entropy generation

depicts from Fig. 9 that an increase in Reynolds number ( $R_e$ ), results higher entropy generation.

### VII. Conclusion

In this article, MHD stagnation point flow of nanofluid over a permeable stretching surface has been investigated. The governing equations such as momentum, energy, and nanoparticle concentration are reduced to ordinary differential equations. The resulting highly coupled nonlinear ordinary differential equations are solved using successive approximation method (SAM). The major outcomes of the present analysis are summarized below:

- It is observed that due to influence of magnetic field, velocity profile increases.
- Brownian motion parameter and thermophoresis parameter shows similar behavior on temperature profile.
- Nano-particle concentration profile decreases due to the increment in Lewis number.

- Entropy generation number increases due to the increment in Brinkmann number and Reynolds number.

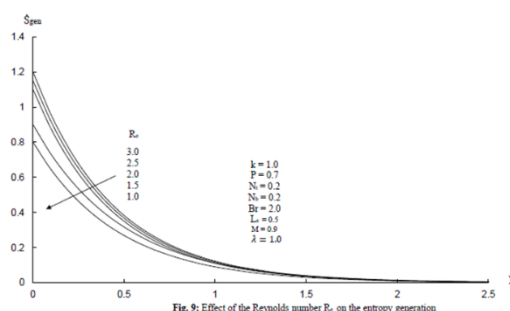


Fig. 9: Effect of the Reynolds number  $R_e$  on the entropy generation

### References

- [1]. B.C. Sakiadis, Boundary-layer behaviour on continuous solid surfaces, *Am. Inst. Chem. Eng. J.* 7 (1961) 26–28.
- [2]. L.E. Erickson, L.T. Fan, V.G. Fox, Heat and mass transfer on amoving continuous moving surface, *Ind. Eng. Chem. Fund.* 5 (1966)19–25.
- [3]. F.K. Tsou, E.M. Sparrow, R.J. Goldstein, Flow and heat transfer in the boundary layer on a continuous moving surface, *Int. J. Heat Mass Transfer* 10 (1967) 219–223.
- [4]. L.J. Crane, Flow past a stretching plate, *Z. Angew. Math. Phys.* 21 (1970) 645–647.
- [5]. P.S. Gupta, A.S. Gupta, Heat and mass transfer on a stretching sheet with suction or blowing, *Can. J. Chem. Eng.* 55 (1977) 744–746.
- [6]. V.M. Soundalgekar, Stokes problem for elastic–viscous fluid, *Rheol. Acta* 13 (1974) 177–179.
- [7]. B. Siddappa, B.S. Khapate, Rivlin–Ericksen fluid flow past a stretching sheet, *Rev. Roum. Sci. Tech. Mech. (Appl.)* 2 (1976) 497–505.
- [8]. L.J. Crane, Flow past a stretching sheet, *Z. Angew. Math. Phys.* 21 (1970) 645– 647.
- [9]. K.R. Rajagopal, T.Y. Na, A.S. Gupta, Flow of a viscoelastic sheet over a stretching sheet, *Rheol. Acta.* 23 (1984) 213–221.
- [10]. W.D. Chang, The non-uniqueness of the flow of viscoelastic fluid over a stretching sheet, *Q. Appl. Math.* 47 (1989) 365–366.
- [11]. B.S. Dandapat, A.S. Gupta, Flow and heat transfer in a viscoelastic fluid over a stretching sheet, *Int. J. Non-Linear Mech.* 24 (1989) 215–219.
- [12]. K. Vajravelu, D. Rollins, Heat transfer in a viscoelastic fluid over a stretching sheet, *J. Math. Anal. Appl.* 158 (1991) 241–255.
- [13]. H.I. Andersson, MHD flows of a viscoelastic fluid past a stretching surface, *Acta. Mech.* 95 (1992) 227–230.
- [14]. J.B.J. Fourier, *Theorie Analytique De La Chaleur*, Chez Firmin Didot, Paris, 1822. [15] C. Cattaneo, *Sulla conduzionedelcalore*, *Atti del Seminario Maermatico e Fisico dell Universita di Modena e Reggio Emilia*, Vol. 3 1948, pp. 83–101.
- [15]. C.I. Christov, On frame indifferent formulation of the Maxwell-Cattaneo model of fi- nite-speed heat conduction, *Mech. Res. Commun.* 36 (2009) 481–486.
- [16]. V. Tibullo, V. Zampoli, A uniqueness result for the Cattaneo-Christove heat conduction model applied to incompressible fluids, *Mech. Res. Commun.* 38 (2011) 77–99.
- [17]. S.H. Han, L.C. Zheng, C.R. Li, X.X. Zhang, Coupled flow and heat transfer in viscoelastic fluid with Cattaneo-Christov heat flux model, *Appl. Math. Lett.* 38 (2014) 87–93.
- [18]. M. Mustafa, Cattaneo-Christove heat flux model for rotating flow and heat transfer of upper convected Maxwell fluid, *AIP Adv.* 5 (2015), <http://dx.doi.org/10.1063/1.4917306>.
- [19]. T. Hayat, M. Farooq, A. Alsaedi, Impact of Cattaneo-Christov heat flux in the flow over a stretching sheet with variable thickness, *AIP Adv.* 5 (2015), <http://dx.doi.org/10.1063/1.4929523>.
- [20]. T. Hayat, M. Imtiaz, A. Alsaedi, S. Almezal, On Cattaneo-Christovheat flux in MHD flow of Oldroyd-B fluid with homogeneous-heterogeneous reactions, *J. Magn. Magn. Mater.* 401 (2016) 296–303.
- [21]. E. R. G. Eckert and R. M. Drake, *Analysis of Heat and Mass Transfer* (McGraw\_Hill, New York, 1972).
- [22]. M. S. Alam and M. M. Rahman, “Dufour and Soret effects on MHD free convective heat and mass transfer flowpast a vertical porous flat plate embedded in a porous medium,” *J. Naval Architect. Marine Eng.* 2 (1), 55–65(2005).
- [23]. A. J. Chamkha and A. Ben\_Nakhi, “MHD mixed convection–radiation interaction along a permeable surfaceimmersed in a porous medium in the presence of Soret and Dufour’s Effects,” *Heat Mass Transfer* 44, 845–856(2008).
- [24]. M. A. Mansour, N. F. El\_Ansary, and A. M. Aly, “Effects of chemical reaction and thermal stratification onMHD free convective heat and mass transfer over a vertical stretching surface embedded in a porous media considering Soret and Dufour numbers,” *Chem. Eng. J.* 145, 340–345 (2008).
- [25]. R. Tsai and J. S. Huang, “Heat and mass transfer for Soret and Dufour’s effects on Hiemenz flow throughporous medium onto a stretching surface,” *Int. J. Heat Mass Transfer* 52, 2399–2406 (2009).
- [26]. O. A. Bég, A. Y. Bakier, and V. R. Prasad, “Numerical study of free convection magnetohydrodynamic heat andmass transfer from a stretching surface to a saturated porous medium with Soret and Dufour effects,” *ComputMater. Sci.* 46, 57–65 (2009).
- [27]. A. V. Kuznetsov and D. A. Nield, “Double-diffusive natural convective boundary layer flow of a nanofluid pasta vertical surface,” *Int. J. Thermal Sci.* 50, 712–717 (2011).
- [28]. W. A. Khan and A. Aziz, “Double-diffusive natural convective boundary layer flow in a porous medium saturated with a nanofluid over a vertical plate: Prescribed surface heat, solutal and nanoparticle fluxes,” *Int. J. Thermal Sci.* 50, 2154–2160 (2011).
- [29]. W. A. Khan, M. J. Uddin and A. I. Md Ismail, “Effect of momentum slip on double-diffusive free convective boundary layer flow of a nanofluid past a convectively heated vertical plate,” *J. Nanoeng. Nanosyst.* 226 (3), 99–109 (2012).
- [30]. F. G. Awad, P. Sibanda, and A. A. Khidir, “Thermodiffusion effects on magneto-nanofluid flow over a stretching sheet, boundary value problem,” 10.1186/1687-2770-2013-136 (2013).
- [31]. W. A. Khan and I. Pop, “Boundary\_layer flow of a nanofluid past a stretching sheet,” *Int. J. Heat Mass Transfer*53, 2477–2483 (2010).
- [32]. J. Buongiorno, “Convective transport in nanofluids,” *ASME J. Heat Transfer* 128, 240–250 (2006).
- [33]. M. Zakaria, "Magnetohydrodynamic viscoelastic boundary layer flow past a stretching plate and heat transfer," *Applied Mathematics and Computation* 155 165–177 (2004).



- [34]. M. Zakaria, "Thermal boundary layer equation for a magnetohydrodynamic flow of a perfectly conducting fluid" *Applied Mathematics and Computation* 148 67–79 (2004).
- [35]. A. Bejan, *Entropy Generation Minimization: The Method of Thermodynamic Optimization of Finite-Size Systems and Finite-Time Processes*, CRC Press, (1995).
- [36]. A. Bejan, A study of entropy generation in fundamental convective heat transfer, *J. Heat Trans.* 101, 718–725 (1979).